Magnetization damping in two-component metal oxide micropowder and nanopowder compacts by broadband ferromagnetic resonance measurements

Jamal Ben Youssef[1] and Christian Brosseau[2,*]

[1]*Laboratoire de Magnétisme de Bretagne (FRE CNRS 2697), Université de Bretagne Occidentale, CS 93837, 6 avenue Le Gorgeu, 29238 Brest Cedex 3, France*

[2]*Laboratoire d'Electronique et Systèmes de Télécommunications (UMR CNRS 6165), Université de Bretagne Occidentale, CS 93837, 6 avenue Le Gorgeu, 29238 Brest Cedex 3, France*

(Received 19 January 2006; revised manuscript received 25 October 2006; published 14 December 2006)

The microwave damping mechanisms in magnetic inhomogeneous systems have displayed a richness of phenomenology that has attracted widespread interest over the years. Motivated by recent experiments, we report an extensive experimental study of the Gilbert damping parameter of multicomponent metal oxides micro- and nanophases. We label the former by *M* samples, and the latter by *N* samples. The main thrust of this examination is the magnetization dynamics in systems composed of mixtures of magnetic (γ-Fe_2O_3) and nonmagnetic (ZnO and epoxy resin) materials fabricated via powder processing. Detailed ferromagnetic resonance (FMR) measurements on *N* and *M* samples are described so to determine changes in the microwave absorption over the 6–18 GHz frequency range as a function of composition and static magnetic field. The FMR linewidth and the field dependent resonance were measured for the *M* and *N* samples, at a given volume fraction of the magnetic phase. The asymmetry in the form and change in the linewidth for the *M* samples are caused by the orientation distribution of the local anisotropy fields, whereas the results for the *N* samples suggest that the linewidth is very sensitive to details of the spatial magnetic inhomogeneities. For *N* samples, the peak-to-peak linewidth increases continuously with the volume content of magnetic material. The influence of the volume fraction of the magnetic phase on the static internal field was also investigated. Furthermore, important insights are gleaned through analysis of the interrelationship between effective permeability and Gilbert damping constant. Different mechanisms have been considered to explain the FMR linewidth: the intrinsic Gilbert damping, the broadening induced by the magnetic inhomogeneities, and the extrinsic magnetic relaxation. We observed that the effective Gilbert damping constant of the series of *N* samples are found to be substantially smaller in comparison to *M* samples. This effect is attributed to the surface anisotropy contribution to the anisotropy of Fe_2O_3 nanoparticles. From these measurements, the characteristic intrinsic damping dependent on the selected material and the damping due to surface/interface effects and interparticle interaction were estimated. The inhomogeneous linewidth (damping) due to surface/interface effects decreases with diminishing particle size, whereas the homogeneous linewidth (damping) due to interactions increases with increasing volume fraction of magnetic particles (i.e., reducing the separation between neighboring magnetic phases) in the composite.

DOI: 10.1103/PhysRevB.74.214413 PACS number(s): 75.75.+a, 76.50.+g, 75.50.Tt

I. INTRODUCTION AND SCOPE

The study of relaxation processes is of widespread interest across different areas of condensed-matter physics, particularly in the irreversible processes of dissipation and decoherence afforded by coupling to an external environment.[1–3] The relationship between the underlying structure of an assembly of magnetic particles and its relaxation behavior is of direct importance to physicists for new theoretical approaches to magnetic dynamics and is crucial for the technologists to develop artificial magnetic structures for major leaps of high density magnetic storage and spintronics technologies, and nanoscale actuators.[4–6] Recent experiments[7] performed on isolated nanoparticles, for which dipole-dipole interactions are predominant, have convincingly shown the validity of Néel's model.[8,9] Unfortunately, even in the simplest case of dipolar interacting ensembles of identical spherical particles no exact results for the magnetic relaxation exist. The study of these systems is further complicated by the distribution of particle sizes, size-dependent anisotropy, aglomeration of the particles, and the presence of exchange interactions between them. We observe that while the magnetic properties of isolated single domain nanoparticles are well understood, it is not clear what effects the long range magnetostatic interactions will have on an assembly of particles. These interactions induce collective behavior between the particles and eventually give rise to complexities that cannot be explained by the Stoner-Wohlfarth theory.[10] The basic equation for describing the local magnetization dynamics in a monodomain ferromagnetic material is the Landau-Lifshitz (LLG) equation of motion with the Gilbert form for the magnetic damping term

$$\partial_t \boldsymbol{M} = -\gamma \boldsymbol{M} \times \boldsymbol{H}_{\text{eff}} + \frac{\alpha}{M_s} \boldsymbol{M} \times \partial_t \boldsymbol{M}. \tag{1}$$

In this continuum theory, $\boldsymbol{M}$ is the magnetization density, with magnitude $|\boldsymbol{M}|=M_s$ equal to the saturation magnetization, γ is the gyromagnetic ratio and is given by $\gamma=\frac{g\mu_B}{\hbar}$, where μ_B is the Bohr magneton moment and the Landé g factor (spectroscopic splitting factor) has value close to the free electron value, i.e., 2, for $3d$ transition metal ferromag-

nets such as Fe and Co, α is the dimensionless Gilbert-damping constant.[10,12] $\boldsymbol{H}_{\text{eff}}$ is the local (effective) magnetic field, which can include magnetostatic fields of external sources, crystal anisotropy, shape-dependent dipolar interactions, and exchange interactions which govern ferromagnetic spin-wave spectral characteristics.[13] Even though the LLG phenomenology captures essential features of the dynamics of magnetization occuring in many condensed matter systems,[11–14] many questions remain still unanswered today due to the complexity of the problem. In particular, Eq. (1) was introduced for small magnetization motions. It is well established that in ultrathin films the linewidths realized are considerably larger than expected from Eq. (1), with α chosen appropriate to high-quality bulk crystalline materials, e.g., see Ref. 15. Another critical element in Eq. (1), the value and physical content of α which describes ill-defined energy dissipation processes, has been elusive, and is still under debate.

On the theoretical front, it should, perhaps be emphasized that there have been several attempts over the last few years to provide a phenomenological description of magnetic damping. One of the main difficulties in deriving the damping term is that various kinds of relaxation processes are melded together in a single damping term. Smith[16] has shown how fluctuation-dissipation arguments can discriminate between alternative phenomenological damping models, e.g., inhomogeneity and finite-size effects, which can complement traditional uniform magnetization descriptions of damped ferromagnetic resonance (FMR). A tensor of damping which reflects the anisotropy of the magnetic system was also derived by Safonov and co-workers.[17]

On the experimental side, many recent studies have been carried out for probing the effects of the local magnetic properties on granular materials. However, predicting the value of α is particular challenge due to a paucity in experimental data.[18–27] From the work of Bhagat and Hirst,[28] it was established that, for pure bulk Ni and hcp Co, α increases significantly for temperatures below 100 K. The origin of this effect was interpreted as arising from magnon-electron scattering interactions characterized by band mixing and Fermi surface deformation. Traditionally, α in thin magnetic films has been studied by measuring the peak-to-peak FMR linewidths.[29–33] For ultrathin magnetic films, α was found to be quite large in comparison with the bulk value.[31] It has to be noted that the anisotropy and porosity mechanisms were treated theoretically by Schlömann,[34] and studied experimentally by many authors.[34,35] Tserkovnyak and co-workers[36] showed that adiabatic spin pumping affects the dynamics of nanoscale ferromagnets and thin films, by renormalizing fundamental parameters such as γ and α, in agreement with experiments.[37] Of most relevance here is the work of Viau *et al.*[38] which revealed that the dynamics of magnetization reversal in magnetically structured granular systems composed of magnetic crystalline grains of a ferromagnetic metal embedded in a nonmagnetic matrix is governed by defects, i.e., impurities, grain boundaries, due to significant changes in the local magnetic interactions. We recently reported a mean-field approach which allows the microwave characterization of a three-dimensional uniform distribution of magnetic grains, with size in the nanometer range, within a nonmagnetic host matrix from measurements of the permeability tensor.[39–42] Reasonable agreement was found between the experimental data and the theoretical predictions obtained using the effective Gilbert damping constant, α, as an adjustable parameter. However, this makes it difficult to isolate the different contributions to the anisotropy and intrinsic damping (i.e., not based on inhomogeneous line broadening effects, but on all other loss mechanisms that take energy out of the spin system).

In this study, we report an extensive and systematic FMR investigation of a series of metallic oxides micro- and nanopowder compacts with varying amounts of magnetic phase in the micro- and nanocomposites. Our main aim in the following is to evaluate from the composition and frequency dependences of the FMR spectra the main magnetic parameters, such as the values of anisotropy and saturation fields. In such experiments, the resonance is probed by sweeping the applied field. The resonance fields provide a measurement of the effective field seen by the uniform precession mode that is excited by a uniform rf field. The effective field, $\boldsymbol{H}_{\text{eff}}$, contains contributions from the external field, the demagnetizing field, the exchange field, the magnetostrictive, and the magnetocrystalline energies. FMR results provide accurate measures of the static properties of magnetic composites, given by anisotropy constants, and the dynamic properties, given by the linewidth ΔH_{pp} of the resonance which provides information on relaxation processes. We have chosen to investigate the magnetic properties of γ-Fe_2O_3/ZnO composites. The choice of this system has been made because chosen γ-Fe_2O_3/ZnO appears as a prototypical member of a class of compounds that possess exceptional microwave properties which make them promising candidates for planar nonreciprocical devices operating at microwave wavelengths.[39–42] Moreover, γ-Fe_2O_3 particles retain important position in magnetic storage media. Furthermore, ZnO is widely used in the manufacture of varistors, and is therefore, of considerable commercial importance. Powder pressing with resin has several advantages over other techniques such as classical sintering and hot-isostatic pressing because of its simplicity, reduced loss of material, low cost, and low-energy consumption. In the present paper, we are primarily interested in the origin of the FMR linewidth in micro- and nanopowder compacts prepared by powder pressing. Since FMR probes local regions differing from each other in the magnetization and/or anisotropy,[43] we expect that due to the polydisperse distribution of the size of powders, the information contained in the resonance line is an average of both the magnetization and anisotropy field. The key observation underlying the work reported here is that the effective magnetic permeability deduced from the analysis of the FMR linewidth is discussed in the framework of a simple mean-field model. In a previous study,[42] we found that the magnetic properties of these nanocomposites are governed by two characteristic features: (i) a much smaller measured value of the reduced remanence ratio than the Stoner and Wohlfarth's prediction concerning randomly distributed single-domain noninteracting particles, and (ii) an increase (respectively, a decrease) of the saturation magnetization (respectively the coercivity) with decreasing aggregate size. These specific properties were ascribed to surface anisotropy.

TABLE I. Selected physical properties of the powders investigated in this study.

Powder	ZnO	ZnO	γ-Fe_2O_3	γ-Fe_2O_3
Average Particle Size[a–c]	1 μm	49 nm	5 μm	23 nm
Powder Color	white	white	purple	brown
Specific Surface Area BET ($m^2\ g^{-1}$)		22		51
Morphology	elongated	elongated	nearly spherical, faceted	nearly spherical, faceted
Crystal Phase	wurtzite	wurtzite	maghemite (cubic spinel)	maghemite (cubic spinel)
Density[a] ($g\ cm^{-3}$)	5.61	5.6	5.24	5.2

[a]From manufacturer product literature.
[b]Determined from specific surface area.
[c]Checked by TEM images.

The influence of the characteristic length scales and geometrical effects inherent to these granular heterostructures on the anisotropy field, magnetic relaxation, and magnetic inhomogeneities is still an open question and has been insufficiently studied.

The layout of the remainder of this paper is as follows. The next section contains a brief description of the experimental technique along with a review of some of the physical properties of the samples studied herein. Section III presents the main experimental results, namely the frequency and concentration dependences of FMR linewidths and the characteristics of intrinsic damping derived from them. The most important results are discussed and compared to some theoretical predictions in Sec. IV. Finally, Sec. V concludes our work with a discussion of directions for future work.

II. MATERIALS AND EXPERIMENTAL DETAILS

Commercially available pure ZnO and γ-Fe_2O_3 (maghemite) powders were used as starting components of the composite materials and had different origins. The micro oxide powders were purchased from Aldrich Chemicals and marked as $\geqslant$99% pure, while the nano oxide powders were supplied from Nanophase Technologies Corp., Burr Ridge, IL. Epoxy resin (Scotchcast 265) purchased from 3M was used as organic binder. Transmission electron microscopy (TEM) was employed to study particle morphology using bright-field micrographs. For that purpose a drop of the suspension of particles dispersed in acetone was placed on a carbon coated Cu grid. The powders were also structurally characterized by x-ray diffraction (XRD) with Cu K_α line in the mode of θ–2θ scan.[44] The γ-Fe_2O_3 particles were nearly spherical with mean diameter about 23 nm, and 5 μm for nano and micro powders, respectively. In order to determine the particle size distribution, large area TEM images were obtained to have better statistics of the particle and were analyzed by the commercial software VISILOG. The γ-Fe_2O_3 (micro and nano) particle size distributions obtained by using more than 300 particles were found to resemble a log-normal distribution. The ZnO crystalline grains were rod shaped with an aspect ratio of about 3:1, and the average equivalent spherical grain size was about 4 9 nm and 1 μm for nano and micro powders, respectively. The particle sizes obtained by the image analysis were consistent with the XRD results. See Table I for details.

In the present study, we have prepared a series of samples with varying composition for the magnetic measurements and consisted of toroids (inner diameter of 3.04 mm, outer diameter of 7 mm, and length of 2 to 4 mm) fabricated using the procedure already described.[42,43] In the following we refer to the samples containing micrometer-sized particles and those containing nanometer-sized particles as *M*-type and *N*-type samples, respectively. See Table II for details. The fractional volume of voids (residual porosity) is deduced knowing the volume fractions of ZnO, Fe_2O_3, and epoxy and was checked by density measurements. Throughout the text, f denotes the volume fraction of Fe_2O_3.

Magnetization measurements were performed using a commercial vibrating sample magnetometer (VSM) cali-

TABLE II. Volume fraction of the different constituents in the *N* and *M* composite samples.

# Sample	γ-Fe_2O_3	ZnO	Epoxy	Porosity
N1	0.55	0	0.12	0.33
N2	0.49	0.05	0.23	0.23
N3	0.40	0.16	0.13	0.21
N4	0.29	0.27	0.24	0.20
N5	0.24	0.32	0.24	0.20
N6	0.18	0.39	0.25	0.18
N7	0.13	0.44	0.25	0.18
N8	0.06	0.51	0.26	0.17
M1	0.64	0	0.14	0.22
M2	0.59	0	0.25	0.16
M3	0.49	0.11	0.25	0.15
M4	0.43	0.17	0.26	0.14
M5	0.31	0.29	0.27	0.13
M6	0.19	0.41	0.27	0.13
M7	0.13	0.48	0.27	0.13
M8	0.07	0.61	0.17	0.15

brated using a nickel disc standard reference material. The measurement of the major hysteresis loops was already discussed.[42] All measurements were done at room temperature.

FMR fields and linewidths were measured at frequencies in the range 6–18 GHz by using a highly sensitive wideband resonance spectrometer with a nonresonant microstrip transmission line. The magnetic field was applied along the toroid axis. During the magnetic field sweeps the amplitude of the modulation field used was appreciably smaller than the FMR linewidth. The amplitude of the exciting field h_{rf} is evaluated to be 16 mOe, which corresponds to the linear response regime.[45] A phase-sensitive detector with a lock-in detection was used. The field derivative of the absorbed power, dP_a/dH, where $P_a=\frac{\omega}{2}\chi''h^2_{rf}$ (χ'' is the imaginary part of the susceptibility of the uniform mode) is proportional to the field derivative $d\chi''/dH$. The resonance field H corresponds to the zero crossing of $d\chi''/dH$ and the FMR linewidth is given by the field interval between the extrema of $d\chi''/dH$. The peak-to-peak FMR linewidth of the uniform resonance mode ΔH_{pp} is related to the damping parameter α and is given by $\Delta H_{pp}=\frac{2\alpha\omega}{\sqrt{3}\gamma}$, where ω is the angular frequency of the exciting field and where the coefficient of $1/\sqrt{3}$ is the correction of the difference between the full width at half maximum and the peak-to-peak linewidth for the Lorentzian line shape. In the current understanding of the mechanisms which contribute to the FMR linewidth a distinction is made between the intrinsic Gilbert damping, the broadening induced by magnetic inhomogeneity, and the extrinsic magnetic relaxation.[46] The different contributions are most conveniently extracted from the relation

$$\Delta H_{pp}=\Delta H_{inhomo}+\Delta H_{homo}=\Delta H_{inhomo}+\frac{2G}{\sqrt{3}\gamma^2 M_s}\omega. \quad (2)$$

The first contribution in the right-hand side of Eq. (2) arises from the broadening induced by magnetic inhomogeneities, e.g., the internal static magnetic field. The second contribution originates from the intrinsic damping. This effect results from a combined effect of exchange interaction and spin-orbit coupling. While the first contribution in Eq. (2) is frequency independent, the second term?is proportional to frequency and can be written in terms of a different Gilbert parameter $G=\alpha\gamma M_s$. Thus, the intrinsic damping is expected to be proportional to G and the frequency dependence of the FMR signal permits to analyze and separate the two contributions in Eq. (2).[15]

In our study, we did not probe how the FMR linewidth depends upon the polarization of the exciting microwave field. The reason for this is that in these preliminary experiments we focused primarily on investigations of the damping for the uniform precessional mode and anisotropy, and not to a detailed study of the shape of the resonance line. When the linewidth is of the same order of the resonance field the analysis would require a much more complex formalism than a single Lorentzian, such as that described in Ref. 47. However, a qualitative analysis of the resonance line shapes indicates that the assumption of a single Lorentzian line is reasonable.

III. LINEWIDTH DATA AND MAGNETIZATION EFFECTIVE DAMPING

A. FMR linewidth

Figures 1(a)–1(d) display a series of absorption (derivative) curves obtained at room temperature, shown in arbitrary units, for four values of f between 0.13 and 0.59. The two different panels correspond to M and N samples. Certain reproducible features can be discerned in these graphs. For the FMR spectra of M samples a weakly resolved line is clearly visible on the low field side which is well separated from the intense and broad FMR line. Overall, the FMR line shapes are quite symmetrical except for the case of $M7$ sample. The main resonance signal is due to a FMR uniform mode which corresponds to a uniform precession of all the magnetic moments coupled to the Fe_2O_3 particles. The origin of the weak signal has yet to be elucidated, but it should be remarked that a similar weak signal (at about 500 Oe) was observed in nanogranular films composed of ferromagnetic amorphous Fe nanoparticles embedded in SiO_2 glass matrices.[48] As the frequency is increased, the uniform mode shifts to a higher field and its strength increases. At this point it is difficult to explain the reasons that cause the distortions of the absorption line at the low volume fraction of magnetic phase for M samples. Such reasons might be variation in the local chemistry[42] and the magnetic inhomogeneity in the sample, e.g., porosity, grain boundaries, grain size distribution, or anisotropy in the randomly oriented crystallites.

The frequency dependence of the peak-to-peak width of the absorption derivative ΔH_{pp} for the M and N samples is shown in Figs. 2(a) and 2(b). Three features characterize these figures: (i) within the experimental error the results for N samples show a linear variation for ΔH_{pp} as the frequency increases [Fig. 2(b)]. It is worth observing that the slope of the lines increases as f is increased; (ii) Fig. 2(a) contains the same type of experimental data as shown in Fig. 2(b), but now for M instead of N samples. The data of Fig. 2(a) show much scatter and do not increase linearly with the increase of frequency; and (iii) it is also noteworthy that the ΔH_{pp} values for N samples are much lower than the corresponding values for M samples. Since the linewidths in polycrystals are generally much larger than in single crystals, this behavior suggests that the FMR linewidth is affected by the presence of magnetic inhomogeneities in the samples.

B. Internal field and magnetization

The next step was to examine the effect of composition on the static internal field. The uniform mode frequency[49] may be obtained in the form

$$\omega_{res}=\gamma(H_{res}+H_{int}), \quad (3)$$

where H_{res} and H_{int} denote the resonance field at frequency, $\frac{\omega_{res}}{2\pi}$, and the internal field, respectively. The resonance frequency for the N and M samples is shown in Figs. 3(a) and 3(b), respectively. In Figs. 3(a) and 3(b) we also compare the H_{res} dependence of the measured main resonance to Eq. (3). It can be seen that the experimental data in Figs. 3(a) and 3(b) are well described by using Eq. (3). Additionally, the

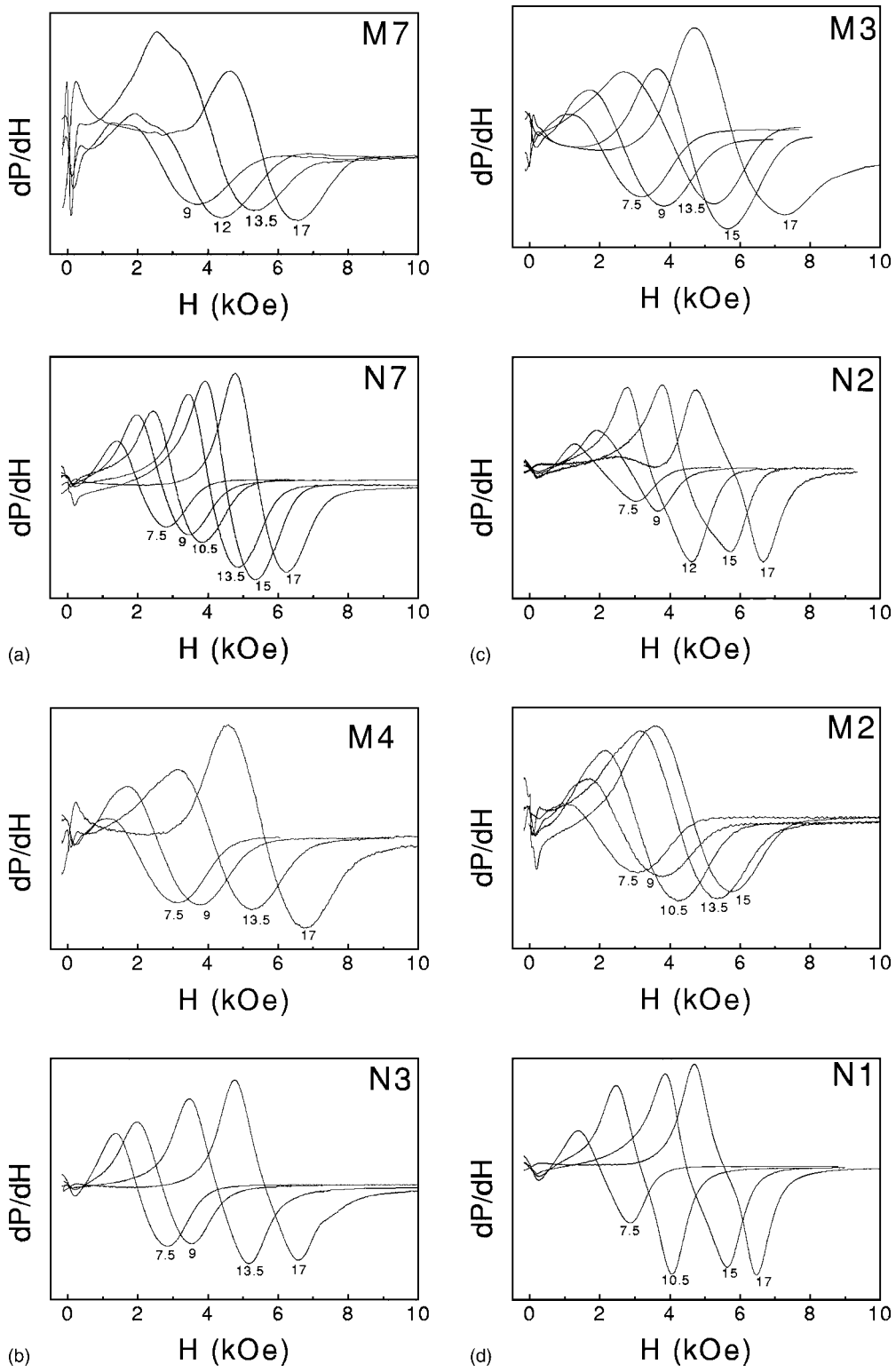

FIG. 1. Variation with magnetic field of the absorbed power derivative at different frequencies for samples considered in the present study. Room temperature. The value of the frequency in GHz is indicated on each curve. The reader should be referred to Table II for the exact values of f. The upper set shows the result for the M sample while the bottom set corresponds to the N sample: (a) $f=0.13$, (b) $f\cong 0.40$, (c) $f=0.49$, (d) $f\cong 0.57$.

slope and offset of the frequency data versus magnetic field appear to be independent of the Fe_2O_3 volume fraction for the N series of samples and are very similar to those found for the M series of samples. The best fit was obtained for $g=2.03$ for all samples, i.e., very close to that of a uniform mode in bulk ferromagnetic Fe material, i.e., $g=2.15\pm0.08$.[49] This is also consistent with the results reported in Ref. 50 where measurements of the g factor of bulk

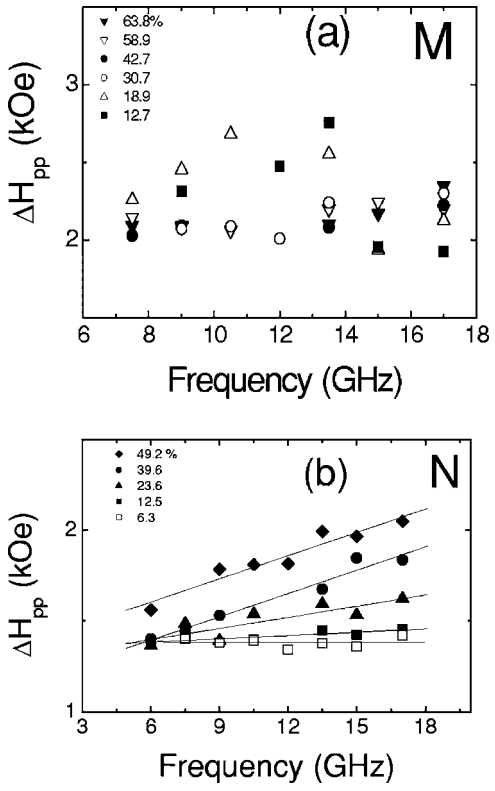

FIG. 2. Frequency dependence of the peak-to-peak linewidth ΔH_{pp}. Room temperature. The values of the volume fractions γ-Fe_2O_3 f are indicated on the diagrams. (a) M samples. (b) N samples. The solid lines serve to guide the eye.

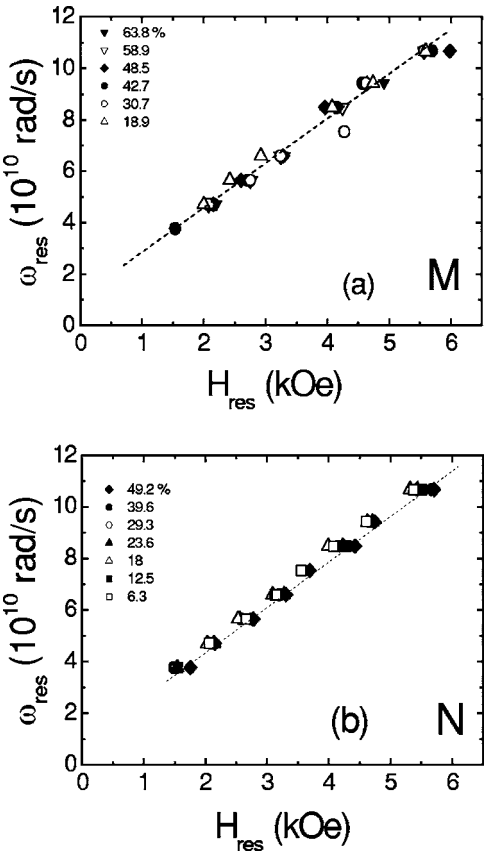

FIG. 3. Dependence of the resonance frequency as a function of the resonance field. Room temperature. Symbols denote the volume fraction of γ-Fe_2O_3. The dashed line is the best fit of the experimental data to Eq. (3). The slope of the line is in the range 17.1–18.1 GHz/kOe for all samples. The corresponding average value of g is 2.03. (a) M samples. (b) N samples.

γ-Fe_2O_3 have been reported in the range from 1.92 to 2.12.

For the sample compositions tested, the values of $4\pi M_s$ obtained from the M vs H cycles performed in a VSM, are shown in Fig. 4. As shown in Fig. 4, the saturation magnetization increases linearly with increasing the content of Fe_2O_3, but we note that the M_s values are typically one order of magnitude smaller for M samples. Qualitatively, these results agree with the fact that M_s increases with increasing interactions. It was noted in Ref. 42 that the increase in magnetization with decreasing particle size is related to the higher surface to volume ratio in a much higher contribution from the surface oxide layer around the particles. In addition, Morales *et al.*[51] have reported a linear correlation between M_s and particle size, suggesting that defects at the particle surface can affect their magnetic properties.

C. Effective permeability

Several authors have suggested that the complex (relative) permeability of an assembly of independent magnetic particles[52] can be evaluated, in the framework of the coarse graining implicit in the use of the effective medium approximation, in the following manner: its real part, in the static limit, is in the form

$$\mu'(\omega \approx 0) = 1 + \frac{4\pi M_s}{H_{\text{eff}}}, \tag{4a}$$

and its imaginary part, at the resonance frequency, is given by

$$\mu''(\omega_{\text{res}}) = \frac{1}{\alpha}\sqrt{\frac{4\pi M_s}{H_{\text{eff}}}}, \tag{4b}$$

where $H_{\text{eff}}=H_{\text{int}}+4\pi M_s$, H_{int} is obtained from Eq. (3), and $\alpha=\frac{\sqrt{3}\gamma\Delta H_{\text{pp}}}{4\pi F}$ at $F=9$ GHz. Figures 5(a) and 5(b) present the γ-Fe_2O_3 volume fraction dependence of $\mu'(\omega\approx 0)$ and $\mu''(\omega_{\text{res}})$ for the M and N samples deduced from Eqs. (4a) and (4b), respectively. It can be seen that the N samples exhibit higher calculated values of $\mu'(\omega\approx 0)$ and $\mu''(\omega_{\text{res}})$ than the corresponding values for the M samples. For comparison we show also the zero-field measurements of $\mu'(\omega \approx 0)$ and $\mu''(\omega_{\text{res}})$ for these samples using the transmission/reflection waveguide method [Fig. 3(c) of our prior work[61]]. Although a limited number of the data points are displayed in Figs. 5(a) and 5(b), we observe that while the agreement between the theoretical and experimental curves of $\mu'(\omega \approx 0)$ is quite reasonable for the M samples (and the N samples for the lowest γ-Fe_2O_3 volume fractions), a quantitative comparison of Eqs. (4a) and (4b) with our experimental results for the N samples at higher γ-Fe_2O_3 volume fractions shows that these equations overestimate (of $\approx$40%) substantially the effective permeability. The largest deviations from this simple model occur for $\mu''(\omega_{\text{res}})$. Therefore, it

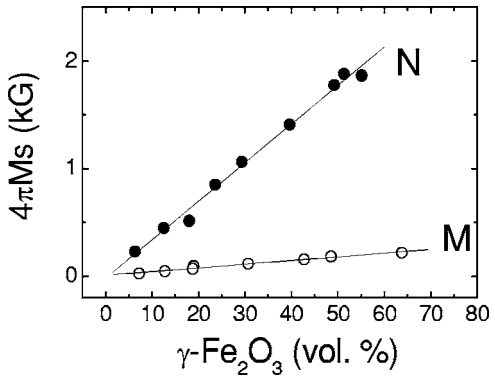

FIG. 4. Saturation magnetization $4\pi M_s$ as a function of the volume fraction of γ-Fe_2O_3. Room temperature. Open circles denote M samples and solid circles represent N samples. The solid lines serve to guide the eye.

seems reasonable to conclude that Eqs. (4a) and (4b) cannot be used to give reliable values for the permeability of the nanocomposites. Likely sources for this discrepancy are the simplicity of the model [since α appears in the denominator of Eq. (4b), a small error in the determination of α will induce a large error in $\mu''(\omega_{res})$] along with the complexity of the system in terms of the magnetic inhomogeneities. In our view, we think that a mean-field (effective) model to take into account both (long-range) magnetostatic intergranular interactions and exchange (short-range) couplings should fail in the case of nanocomposites.[38,39,42,53] This point will be discussed in more detail in Sec. IV.

D. Magnetic effective damping and peak-to-peak linewidth

We now turn our attention to the determination of the effective Gilbert damping parameter. In Fig. 6(a), we plot the γ-Fe_2O_3 volume fraction dependence of α deduced from the spectral dependence of the peak-to-peak linewidth ΔH_{pp}, i.e., Eq. (2), for the N samples. The data follow an upward linear trend with increasing f. These data should be compared to the values obtained by fitting the shape of the gyromagnetic resonance line using the LLG equation and α being treated as an adjustable parameter of the shape of the permeability spectrum.[42] One can clearly see from this figure that α obtained from permeability measurements is found to be more than 1.5 times higher than the typical α value measured with FMR. In order to understand how size of the magnetic particles influences the damping parameter, it is also desirable to compare the values of α for the N and M samples. This is done in Fig. 6(b). We would like to note that the behavior for α for the N samples is linearly increasing when f is increased in contrast to the M counterparts.

To complete the analysis of the features of the effective damping parameter for the M and N samples, we compared in Figs. 7(a) and 7(b) the two contributions in the peak-to-peak linewidth, i.e., ΔH_{inhomo} and ΔH_{homo}, assuming that the inhomogenous contribution of ΔH is independent of frequency and the homogeneous contribution of ΔH depends linearly on frequency, as expressed by Eq. (2). The key difference between the two types of samples is that while

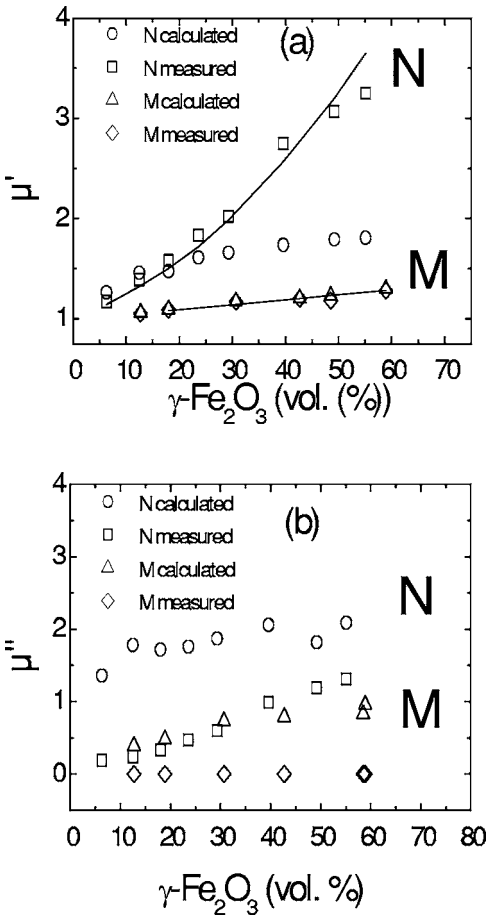

FIG. 5. Comparisons of experimental with calculated values of the complex effective (relative) permeability as a function of the volume fraction of γ-Fe_2O_3. Room temperature. Squares and diamonds denote the experimental values for the N samples and M samples, respectively Ref. 42. Circles and triangles denote the calculated values for the N samples and M samples, respectively. The calculated values were obtained from Eqs. (4a) and (4b), respectively. (a) Real part of the effective permeability, in the static limit. The experimental data are for 0.2 GHz. The solid lines are best-fit expectations from Bruggeman equation to the experimental data ($\mu'_{1M}=1.5$, $\mu'_{1N}=7.5$, and $\mu'_2=1$); see Sec. IV C for details. (b) Imaginary part of the effective permeability, at the resonance frequency.

ΔH_{homo} increases as f is increased, ΔH_{inhomo} is nearly constant over the range of composition explored. As can be seen from Figs. 7(a) and 7(b), $\Delta H_{homo} \ll \Delta H in_{homo}$, reflecting the central role of inhomogeneities in the relaxation process for M samples. Another interesting observation that can be readily made from these figures is that the increasing dependences of ΔH_{homo} versus f for the M and N samples are pretty close to each other.

Finally, results for the values of $G=\alpha_{homo}\gamma M_s$ as a function of f are displayed in Fig. 8. It is found to increase with increasing the volume fraction of the magnetic component. Again, the results display large differences between the N and M samples.

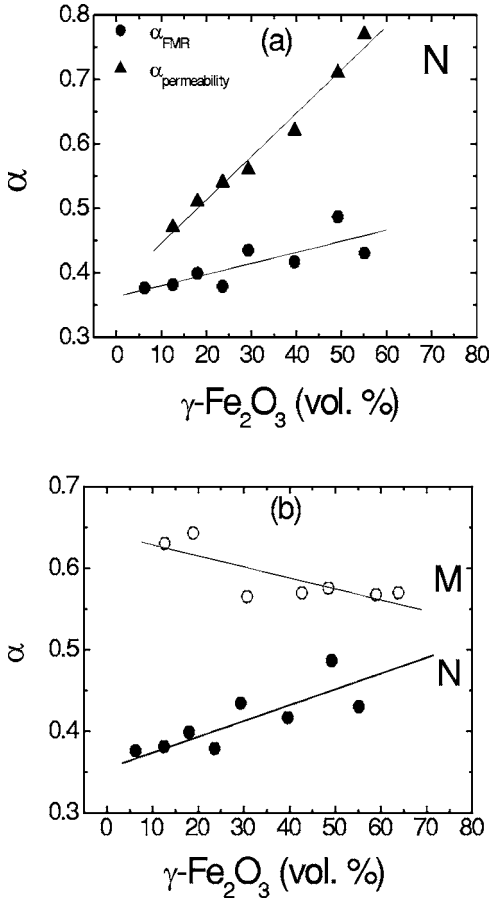

FIG. 6. The Gilbert damping constant α as a function of the volume fraction of γ-Fe_2O_3. Room temperature. The solid lines serve to guide the eye. For the determination of α from the FMR we use γ=17.8 GHz/kOe corresponding to g=2.03. (a) Comparison of the experimental values of α determined by FMR (full circles) with those determined by the fit of the effective permeability using the Landau-Lifshitz-Gilbert model (full triangles) [Ref. 42]. (b) Comparison of the experimental values of α determined by FMR for N (open circles) and M (full circles) samples.

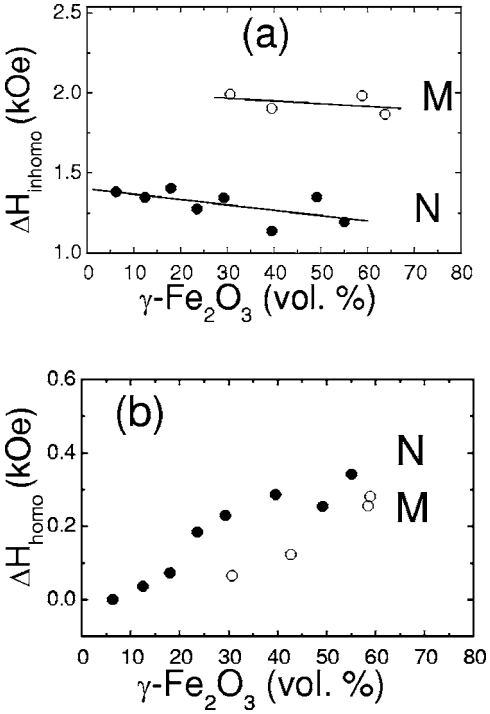

FIG. 7. Comparison of the values of the peak-to-peak linewidths, ΔH_{inhomo}, and, ΔH_{homo}, for N (full circles) and M (open circles) samples as a function of the volume fraction of γ-Fe_2O_3. Room temperature. The solid lines serve to guide the eye. (a) inhomogenous contribution, independent of frequency [see Eq. (2)]. (b) homogeneous contribution, proportional to frequency [see Eq. (2)].

IV. FURTHER DISCUSSION

A. FMR linewidth

As noted by a number of authors, a central difficulty in the measurement of magnetization damping by FMR is that experimental values of the FMR linewidth reflect the effects of inhomogeneity in addition to the intrinsic damping.[21,22,24] The extrinsic magnetic relaxation, which contributes to the FMR linewidth, has been argued to originate from the coupling between the uniform resonance mode and degenerate spin waves through structural inhomogeneity, i.e., two-magnon scattering process.[4] However, up to now the differences between intrinsic and extrinsic magnetic relaxations have not been clearly analyzed and discerned from the frequency dependence of the linewidth in magnetic granular nanophases.

It is worth recalling that some experimental studies in systems of magnetic nanoparticles at different temperatures show that the line shape of the FMR spectra remains symmetric in the whole range of temperatures.[33,37] The apparent asymmetry and structure of the peak absorption line for the M samples are interesting features of this study. One possibility for explaining this might be the nonuniform magnetization motions due to the orientation distribution of the local anisotropy fields. Under such circumstances the absorption line tends to acquire an asymmetrical pattern inherent to a

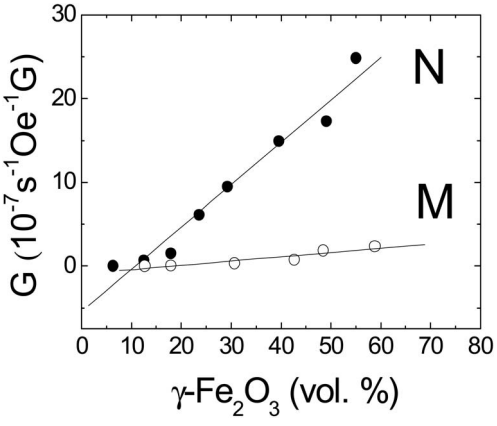

FIG. 8. Comparison of the values of the parameter $G = \alpha_{homo} M_s \gamma$ for N (full circles) and M (open circles) samples as a function of the volume fraction of γ-Fe_2O_3. For the determination of G we use γ=17.8 GHz/kOe corresponding to g=2.03 and the values of M_s taken from the data of Fig. 4. Room temperature. The solid lines serve to guide the eye.

randomly oriented system of magnetically anisotropic grains. Parenthetically, it is worth observing that two-maxima absorption curves have been predicted by Raikher and Stepanov[53] in their analysis of FMR in suspensions of ferromagnetic particles. It could be also argued that there are modes associated with grain size polydispersity which are close to the frequency of the dominant mode.[38] These weaker modes may significantly distort the line shape of the dominant mode. More complete FMR studies of this frequency region with monodisperse distributions of particles are needed to resolve this issue. Our measurements show that for the *N* samples the line broadens with increasing Fe_2O_3 content while the *M* samples do exhibit a decrease in linewidth with increasing Fe_2O_3 content. This suggests that: (i) the broadening of the FMR linewidth in the *N* samples studied is due to both the polydispersity and the dynamic magnetic inhomogeneity of the samples, e.g., excess spins in oxide layers,[54] and (ii) the linewidth broadening mechanisms are not the same for these two types of samples. In addition, the relatively large porosities (see Table I) can make a significant contribution to the linewidth. Note that nonuniform stress fields generated during the fabrication process can be responsible for the eventual nucleation, evolution, and coalescence of voids. A previous study by Golub and co-workers[43] discussed also a mechanism of line broadening in terms of static fluctuations of the random internal fields on grains.

B. Effective Gilbert damping parameter

As we have already noticed in the introductory part of this paper, there is likely to be a complex interaction between existing sources of relaxation for spins. Magnetism in nanophases has attracted a great deal of interest, as the physical dimensions involved are comparable to certain characteristic length scales. In this context we note that several authors have proposed mechanisms that can account for reduced coercivity beyond that expected from Stoner-Wohlfarth model. One natural explanation would be that the exchange coupling between neighboring magnetic grains dominate the demagnetizing and magnetocrystalline anisotropy energies in the material.[55] However, one has no rigorous calculation of the characteristic length scale on which this process ought to proceed. For collections of well-separated uniformly shaped single domain, the magnetocrystalline and shape anisotropies of the grains are only present. In a random distribution of very fine particles embedded in a nonmagnetic matrix, interparticle interactions are dipolar and exchange in nature.[56,57] In our earlier study,[42] it was suggested that the epoxy coating can affect the intrinsic properties of the Fe_2O_3 particles aggregates,[58] and the decreased coercivity was attributed to dipole interaction between the magnetic particles which are separated by thin nonmagnetic layers. If intergranular exchange coupling is dominant the aggregate size should be larger than the magnetostatic-exchange length $\lambda_{ex} \propto \sqrt{\frac{A}{M_s^2}}$, where *A* is the exchange stiffness constant, and the magnetocrystalline-exchange length $\sqrt{\frac{A}{K}}$, where *K* is the anisotropy constant. For the nanocomposite media of current interest, an order-of-magnitude estimate of λ_{ex} is typically 20–30 nm or so. This value is consistent with the mean aggregate size below which a significant reduction in coercivity is observed.[42] The shape anisotropy is much larger than the magnetocrystalline anisotropy, so that the effective anisotropy is essentially equal to the shape anisotropy and the range of perturbation is of the order of λ_{ex}. The average aggregate size exceeds significantly the single-domain radius which is estimated to be $\cong 5-10$ nm. However, particles in an aggregate are considered to be tightly exchange coupled, and aggregates may be treated as having a single uniform magnetization. The prominent intergrain exchange couplings that play a dominant role when reducing the particle size and the separation distance between neighboring particles, i.e., increasing the volume fraction of Fe_2O_3 particles, to approximately λ_{ex} induce two things: (i) a bulk (effective) value of the effective damping parameter $\alpha \sim 10^{-1}$ which is much larger than the intrinsic damping parameter for typical transition metal ferromagnets $\alpha < 10^{-2}$, [Refs. 2, 10, 38, and 59] and (ii) an effective magnetic permeability for nanocomposites that can be much larger than the magnetic permeability of composites containing large particle sizes. It is also worth observing that Löffler *et al.*[60] have pointed out that magnetic correlations in nanostructured magnets extend over many grains with a minimal correlation length at grain sizes of the order of a domain-wall width.

One more thing calls for attention. The interest in the problem of magnetization mechanisms of nanophases was excited by the pioneering work of Aharoni[61] who recognized the role of grain size and composition in exchange modes. The theory, concerning small ferromagnetic spheres, is valid when the magnetostatic energy is small compared to the exchange energy and predicts that the resonance frequency depends on the roots of a the derivatives of the spherical Bessel functions, and is $\propto R^{-\beta}$, where *R* is the radius of the sphere and $\beta \cong 0.66$ for spheres having strong surface anisotropy or $\beta = 2$ if the particle size or the surface anisotropy is considerably reduced. It was also suggested that at granular interfaces, the reduced grain-boundary exchange contributes to the perturbation of the spin structure and defines an effective intergranular exchange.[62] It should be noted that the extension of the earlier theories of magnetostatic modes of ferromagnetic spheres to include exchange as well as dipolar interactions needs to be addressed in detail.

C. Mean-field calculation of permeability

Let us now discuss the issue of effective magnetic permeability of these granular composites. For many years the mean-field (effective medium) approximation has provided the much needed handle on the difficult problem of approximating the composition dependence of the physical properties of heterostructures. Numerous approaches[42,53] to modeling of the effective permeability in a disordered composite have been attempted, e.g., Bruggeman, McLachlan. Generally speaking, continuum modeling allows investigation of the microstructural behavior at the relevant long length scales. Material-specific behavior is incorporated through the permeability and volume fraction of each constituent in the mixture.

The Bruggeman model was chosen for comparison with experimental data because it is generally acknowledged to be

a reasonable predictor for effective properties of composites in granular form, and it is simple to derive closed form relations for many properties.[42,63] In this self-consistent mean-field permeability model the particles of any single material component are assumed to be embedded in an effective medium with permeability equal to the effective permability μ that we are trying to find. Here the effective medium consists of an assembly of randomly oriented crystalline spherical grains. For the magnetic-nonmagnetic composites of interest in this paper, the standard Bruggeman symmetric effective-medium analysis yields

$$f\frac{\mu_1-\mu}{\mu_1+2\mu}+(1-f)\frac{\mu_2-\mu}{\mu_2+2\mu}=0, \tag{5}$$

where μ_1 denotes the Fe_2O_3 relative permeability and $\mu_2=1-j0$. In this way of thinking the procedure amounts to finding the roots of a second-order polynomial and the physical root of Eq. (5) is determined from requirements of positivity of μ' and μ''.

For our model calculations, we have fitted Eq. (5) to the experimental data shown in Fig. 6 by treating μ_1 as an adjustable parameter. The corresponding best fits of the γ-Fe_2O_3 permeability of the *M* and *N* samples were: $\mu'_{1M}=1.5$ and $\mu'_{1N}=7.5$, respectively. Our calculations as summarized in Fig. 5(a) show that the simulations reproduce the actual features of the data reasonably well, which is the monotonic rather rounded increase of the permeability as the volume fraction of the magnetic component is increased. However, there is significant discrepancies [solid line in Fig. 5(a)] between experimental and calculated values, especially for $f>0.25$. We note that the value of the microwave intrinsic permeability μ_1 are comparable to those found in related material systems, e.g., Refs. 38 and 64.

We conclude by briefly making a point related to the modeling of data in Fig. 5(a) by the conventional Bruggeman model for describing the microwave properties of magnetic-insulating medium mixtures.[65] Five limitations of this model deserves particular attention: (i) both components in the magnetic-nonmagnetic composite are treated in a fully equivalent way; (ii) it assumes that the mixture is made of two types of spherical inclusions which provide the least surface area and must therefore occupy a more appreciable fraction of the total volume before guaranteeing enough contact for the existence of percolation pathways. While γ-Fe_2O_3 particles are nearly spherical, ZnO particles are nonspherical (rod shaped), thus shape and surface anisotropy can play an important role at diameters below a few hundred nanometers; (iii) it does not take into account the important epoxy-coated structure; (iv) it assumes that only the volume fraction of the constituents are relevant. However, for assemblies of nanophases where distributions of particle sizes, shapes, and defects render the interpretation quite difficult, we expect that order parameters different from these volumic parameters are needed for a proper description of surface/interface effects on the magnetic anisotropy and permeability; and (v) in the long-wavelength limit, it is not particle size dependent. Compared with the micrometer-size γ-Fe_2O_3 particles, the γ-Fe_2O_3 nanoparticles are not only of small size, but have different crystal and domain structures.[7] Thus, they exhibit different microwave magnetic properties. Great care must be taken when interpreting dynamical properties in magnetic environments containg multiple length scales, because these properties are governed by several interacting processes taking place simultaneously at different length scales. For dynamical simulations, the relevant length scales should be coupled. A step forward in this direction has been given recently by Dobrovitski *et al.*,[66] and Löffler *et al.*[60] There is even debate concerning the fact that the analysis of magnetic correlations cannot be reconciled with a mean-field description.[67] It is also worth recalling that it has been recognized that to fully understand this phenomenon it is essential to first understand granular packing in particulate assemblies. Our use of these model calculations is somewhat different from that of Ramprasad *et al.*[63] who have recently reported similar model calculations. It is interesting to observe that a set of bounds for the effective permeability of composites containing spherical (monodisperse) particles with a ligand shell coating was derived by these authors,[63] showing that this physicochemical attribute of the particles may become relevant when the ligand shell thickness is large compared to the particle radius. It was also emphasized by these authors[63] that eddy current losses of composites consisting of ferromagnetic (monodisperse) particles embedded in a nonmagnetic matrix are negligible below 10 GHz, if the particle radii are smaller than 100 nm, while composites with larger particles display significant effective permeability degradation.

Another aspect which deserves attention is the issue of percolation in granular solids. It was suggested that in such materials the magnetic phase forms an infinite network enclosing isolated regions of the nonmagnetic phase, exhibiting enhanced magnetic properties since the magnetic closure structure is facilitated.[68] A salient feature of percolation is that it is governed by a single order parameter, i.e., the critical threshold, and thus provides a stringent test for identifying this transition. Here it is interesting to point out that the γ-Fe_2O_3 volume fraction above which significant discrepancies [Fig. 5(a)] can be observed between the experimental and calculated values of the real part of the static effective permeability using Eq. (4a) is slightly higher than the threshold of three-dimensional continuum percolation predicted by Scher and Zallen, i.e., $\cong 0.17$ [Ref. 69]. However, our data cannot prove that the increase in effective permeability is associated with a static percolation transition when γ-Fe_2O_3 nanophases form a system-spanning cluster. This remark is consistent with our previous findings.[42]

V. SUMMARY AND ADDITIONAL REMARKS

To summarize, we have used FMR at microwave frequency to parametrize changes in the magnetic relaxation in randomly mixed γ-Fe_2O_3/ZnO composite samples as a function of composition and particles size. In this work and our earlier work,[42] we presented a series of measurements which provide important insights into the magnetization behavior of nano- and microsized magnetic granular materials at microwave frequencies. We have made two contributions with this

paper. The first one consists in carefully evaluating the FMR spectra of fine powdered specimens of iron oxides dispersed in a nonmagnetic matrix. A comparison of the measured FMR between magnetic granular micro- and nanocomposites has not, so far as we know, been reported before, thus the results in Figs. 1(a)–1(d). Our second contribution deals with the damping mechanisms of these heterostructures. We have studied the dependence of the effective Gilbert damping parameter and the different contributions to the peak-to-peak FMR linewidth of the uniform resonance mode as a function of magnetic particle size and volume fraction of the magnetic phase. The inhomogeneous linewidth (damping) due to surface/interface effects decreases with diminishing particle size, whereas the homogeneous linewidth (damping) due to interactions increases with increasing volume fraction of magnetic particles (i.e., reducing the separation between neighboring magnetic phases) in the composite.

Upon closing a few remarks are in order. The most intriguing open questions concern the nature of the magnetic damping of an assembly of fine magnetic particles, and an understanding of the microwave response characteristics of magnetic heterostructures for all temperatures, magnetizations, and magnetic fields. Since the damping mechanism is expected to be electronic in origin, and sensitive to the interaction of electrons with the interfaces, a frequent question in magnetization dynamics is whether there is more than one (isotropic) damping term. According to recent theoretical works,[17,57] it has been suggested that more complicated forms of phenomenological (anisotropic) damping with a "hierarchy of dissipative terms" could be at play, a matter currently far from settled. Clearly the role of intrinsic and extrinsic factors in the microwave loss process in nanomaterials is just beginning to be uncovered.

To understand the precise nature of the magnetic damping mechanism, another fundamental problem must be addressed. In the continuum theory used in Sec. IV, the only dependence of the magnetic permeability with the constituent appears through the volume fraction. Each material point in the continuum theory represents the coarse-grained magnetic behavior of its micro- (or more appropriately nano) constituent. From a statistical physics point of view, the coarse-grained behavior of a suitably large, statistically representative number of atoms and grains is represented by the usual effective property of the material. At length scales where the discrete nature of matter becomes apparent, additional physical phenomena not readily included in the classical continuum magnetostatics framework become important. If there are such effects, the typical coarse-graining implicit in the use of the effective magnetic permeability becomes inadequate. Thus, on physical grounds, one can expect that magnetization/field at a point at the nanoscale should depend on the magnetic state of all surrounding neighborhood points rather than the state just at that point (as assumed by classical magnetostatics). Over the past decade, use of micromagnetic (MM) theory to explore the macroscopic magnetic properties of nanocrystalline materials has grown in tandem with the increase in accessible computing power to do such calculations. There have been a number of recent MM simulation studies of how the spin structure is modified at granular interfaces. These include investigations by Herzer,[54] Chopra and Hua,[70] and Tsymbal *et al.*[71] Work is now in progress to investigate nonuniform distributions of magnetization and demagnetizing field in nanometric systems by MM calculations.[17] An additional verification is essential since mean-field calculations (continuum theories) are shown to have their limitations.

Finally, we emphasize that nanomagnetism is in the midst of an explosive period of discovery and deepening understanding, made possible by new technology and new ideas. The study of magnetic structures on the submicrometer and nanometer length scales has captured the attention of a number of authors recently because of its relevance in the context of spin electronics,[72–78] high density magnetic recording,[79] magnetic random access,[80] and monolithic microwave integrated circuit applications.[81] Future work will concentrate on optimizing the densification of the nanoparticles into a bulk material while retaining the nanostructure of magnetic phases of 3*d* elements- Fe, Co, and Ni. Furthermore, the results presented in this paper have significant implications for dynamical models of magnetization in nanophases. However, additional measurements and theoretical interpretation are required to generalize these promising initial results.

ACKNOWLEDGMENTS

The authors are indebted to N. Vukadinovic who critically read this manuscript and made several useful suggestions. Thanks are also due to A.-M. Konn for her help in the preparation of the materials.

*Author to whom correspondence should be addressed. Also at the Département de Physique, Université de Bretagne Occidentale. Email address: brosseau@univ-brest.fr

[1] P. M. Chaikin and T. C. Lubenski, *Principles of Condensed Matter Physics* (Cambridge University, Cambridge, England, 1995).

[2] H. B. Callen, *Fluctuation, Relaxation and Resonance in Magnetic Systems*, edited by D. Ter Haar (Plenum, New York, 1961). See also C. Warren Haas and H. B. Callen, *Magnetism*, edited by G. T. Rado and H. Suhl (Academic, New York, 1963), Vol. 1.

[3] J. L. Simonds, Phys. Today **48** (4), 26 (1995).

[4] M. Sparks, *Ferromagnetic-Relaxation Theory* (McGraw-Hill, New York, 1964); M. Sparks, R. Loudon, and C. Kittel, Phys. Rev. **122**, 791 (1961).

[5] C. E. Patton, in *Magnetic Oxides*, edited by D. J. Craik (Wiley, London, 1975), Chap. 10, pp. 575–645.

[6] C. W. Haas and H. B. Callen, in *Magnetism* (Academic, New York, 1963), Vol. 1, Chap. 10.

[7] W. Wernsdorfer, E. B. Orozco, K. Hasselbach, A. Benoit, B. Barbara, N. Demoncy, A. Loiseau, H. Pascard, and D. Mailly, Phys. Rev. Lett. **78**, 1791 (1997).

[8] L. Néel, Ann. Geophys. (C.N.R.S.) **5**, 99 (1949).
[9] W. F. Brown, Jr., Phys. Rev. **130**, 1677 (1963).
[10] A. Aharony, *Introduction to the Theory of Ferromagnetism* (Oxford University Press, New York, 1996). See also E. C. Stoner and E. P. Wohlfarth, Philos. Trans. R. Soc. London **240**, 599 (1948); and A. H. Morrish, *The Physical Principles of Magnetism* (Wiley, New York, 1965).
[11] See, T. L. Gilbert, Phys. Rev. **100**, 1243 (1955); L. Landau and E. Lifshitz, Phys. Z. Sowjetunion **8**, 153 (1935). See also L. D. Landau, E. M. Lifshitz, and L. P. Pitaevski, *Statistical Physics*, 3rd ed. (Pergamon, Oxford, 1980), Part 2; L. D. Landau, *Collected Papers*, edited by D. ter Haar (Gordon and Breach, New York, 1967); R. Kikuchi, J. Appl. Phys. **27**, 1352 (1956).
[12] W. F. Brown, Jr., *Micromagnetics* (Wiley-Interscience, New York, 1963); H. Kronmüller and M. Fähnle, *Micromagnetism and the Microstructure of Ferromagnetic Solids* (Cambridge University Press, Cambridge, U. K., 2003). See also the public domain Object Oriented MicroMagnetic Framework (OOMMF) micromagnetic package, developed at the National Institute of Standards and Technology, for simulations, i.e., M. J. Donahue and D. G. Porter, *OOMMF User's Guide*, Version 1.0, NIST Interagency Report No. NISTIR 6376, Sept 1999, National Institute of Standards and Technology, Gaithersburg, MD, 1999; http://math.nist.gov/oommf/. The solver imposes 3D spins on a 2D grid of squares to simulate distributions of particles. Details can be found in M. J. Donahue and R. D. McMichael, Physica B **233**, 272 (1997);and M. J. Donahue, D. G. Porter, R. D. McMichael, and J. Eicke, J. Appl. Phys. **87**, 5520 (2000). However, despite recent advances in simulation methodology and algorithm, computational speed continues to dictate the level of complexity that one can practically study in modeling "real" materials.
[13] W. F. Brown, *Magnetostatic Principles in Ferromagnetism* (North-Holland, Amsterdam, 1962).
[14] N. A. Usov and S. E. Peschany, J. Magn. Magn. Mater. **130**, 275 (1994).
[15] Z. Celinski and B. Heinrich, J. Appl. Phys. **70**, 5935 (1991). See also P. W. Brouwer, Phys. Rev. B **58**, R10135 (1998).
[16] N. Smith, J. Appl. Phys. **92**, 3877 (2002). This article showed that recently proposed alternatives (Safonov, Safonov and Neal Bertram, see Ref. 37) to the Gilbert damping model may lead to physically untenable predictions or contradictions.
[17] V. L. Safonov, J. Magn. Magn. Mater. **195**, 526 (1999); J. Appl. Phys. **85**, 4370 (1999). See also V. L. Safonov and H. Neal Bertram, *ibid.* **87**, 5681 (2000); V. L. Safonov and H. Neal Bertram, in *The Physics of Ultra-High-Density Magnetic Recording*, edited by M. Plumer, J. van Elk, and D. Weller (Springer, Berlin, 2001), p. 81; and V. L. Safonov and H. Neal Bertram, Phys. Rev. B **71**, 224402 (2005).
[18] M. Farle, Rep. Prog. Phys. **61**, 755 (1998).
[19] B. Heinrich, K. B. Urquhart, A. S. Arrott, J. F. Cochran, K. Myrtle, and S. T. Purcell, Phys. Rev. Lett. **59**, 1756 (1987). See also B. Heinrich, J. F. Cochran, M. Kowalewski, J. Kirschner, Z. Celinski, A. S. Arrott, and K. Myrtle, Phys. Rev. B **44**, 9348 (1991).
[20] B. R. Pujada, E. H. C. P. Sinnecker, A. M. Rossi, and A. P. Guimaraes, Phys. Rev. B **64**, 184419 (2001).
[21] R. S. de Biasi and T. C. Devezas, J. Appl. Phys. **49**, 2466 (1978).
[22] K. Nagata and A. Ishihara, J. Magn. Magn. Mater. **104-107**, 1571 (1992).
[23] R. E. Camley and D. L. Mills, J. Appl. Phys. **82**, 3058 (1997) and references to earlier work cited therein.
[24] R. E. Camley, J. Magn. Magn. Mater. **200**, 583 (1999).
[25] U. Ebels, L. D. Buda, K. Ounadjela, and P. E. Wigen, in *Spin Dynamics in Confined Magnetic Structures I*, edited by B. Hillebrands and K. Ounadjela (Springer-Verlag, Berlin, 2002).
[26] R. D. Sanchez, M. A. Lopez-Quintela, J. Rivas, A. Gonzales-Penedo, A. J. Garcia-Bastida, C. A. Ramos, R. D. Zyaler, and S. Ribeiri Guevara, J. Phys.: Condens. Matter **11**, 5643 (1999).
[27] C. Surig and K. A. Hempel, J. Appl. Phys. **80**, 3426 (1996).
[28] S. M. Bhagat and L. L. Hirst, Phys. Rev. **151**, 401 (1966); Phys. Rev. B **10**, 179 (1974). See also S. M. Bhagat and P. Lubitz, Phys. Rev. B **10**, 179 (1974); P. Lubitz, S. F. Cheng, F. J. Rachford, M. M. Miller, and V. G. Harris, J. Appl. Phys. **91**, 7783 (2002); and F. Schreiber, J. Pflaum, Z. Frait, Th. Mühge, and J. Pelzl, Solid State Commun. **93**, 965 (1995).
[29] B. Heinrich and J. F. Cochran, Adv. Phys. **42**, 523 (1993).
[30] W. Platow, A. N. Anisimov, G. L. Dunifer, M. Farle, and K. Baberschke, Phys. Rev. B **58**, 5611 (1998).
[31] S. Mizukami, Y. Ando, and T. Miyazaki, J. Magn. Magn. Mater. **239**, 42 (2002); S. Mizukami, Y. Ando, and T. Miyazaki, Phys. Rev. B **66**, 104413 (2002).
[32] N. Vukadinovic, J. Ben Youssef, H. Le Gall, and J. Ostorero, Phys. Rev. B **62**, 9021 (2000). See also N. Vukadinovic, M. Labrurne, J. Ben Youssef, A. Marty, J. C. Toussaint, and H. Le Gall, *ibid.* **65**, 054403 (2001).
[33] R. Urban, G. Woltersdorf, and B. Heinrich, Phys. Rev. Lett. **87**, 217204 (2001).
[34] E. Schlömann, J. Phys. Chem. Solids **6**, 242 (1958).
[35] C. E. Patton, Phys. Rev. **179**, 352 (1969). See also P. Röschmann, IEEE Trans. Magn. **14**, 1247 (1975).
[36] Y. Tserkovnyak, A. Brataas, G. E. W. Bauer, and B. I. Halperin, Rev. Mod. Phys. **77**, 1375 (2005).
[37] S. Mizukami, Y. Ando, and T. Miyazaki, J. Magn. Magn. Mater. **226**, 1640 (2001).
[38] G. Viau, F. Ravel, O. Acher, F. Fiévet-Vincent, and F. Fiévet, J. Magn. Magn. Mater. **140-144**, 377 (1995). See also P. Toneguzzo, O. Acher, G. Viau, F. Guillet, E. Bruneton, F. Fievet-Vincent, and F. Fievet, J. Appl. Phys. **81**, 5546 (1997); and P. Toneguzzo, G. Viau, O. Acher, F. Guillet, E. Bruneton, F. Fievet-Vincent, and F. Fievet, J. Mater. Sci. **35**, 3767 (2000).
[39] C. Brosseau, S. Mallegol, P. Queffelec, and J. Ben Youssef, Phys. Rev. B **70**, 092401 (2004).
[40] S. Mallegol, C. Brosseau, P. Queffelec, and A.-M. Konn, Proceedings of the International Conference on Magnetism 2003, Roma, Italy (unpublished). See also S. Mallegol, C. Brosseau, P. Queffelec, and A.-M. Konn, J. Magn. Magn. Mater. **272**, 1518 (2004).
[41] S. Mallegol, C. Brosseau, P. Queffelec, and A. M. Konn, Phys. Rev. B **68**, 174422 (2003).
[42] C. Brosseau, J. Ben Youssef, P. Talbot, and A. M. Konn, J. Appl. Phys. **93**, 9243 (2003). XRD of nanometric and micrometric Fe_2O_3 powders showed a high purity material for the nanometric particles while for the micrometer-sized particles it was found a certain amount of Fe_3O_4 impurities that was estimated to be in the vol % range.
[43] V. O. Golub *et al.*, Mater. Sci. Forum **373-376**, 197 (2001). V. O. Golub, G. N. Kakazei, and N. A. Lesnik, in *Frontiers in Magnetism of Reduced Dimension Systems*, edited by V. G. Bar'yakthar, P. E. Wigen, and N. A. Lesnik, NATO ASI Series 3,

High Technology (Kluwer, Dordrecht, 1998), Vol. 49, pp. 211–216.
[44] P. Talbot, A.-M. Konn, and C. Brosseau, J. Magn. Magn. Mater. **249**, 483 (2002).
[45] B. E. Argyle, W. Jantz, and J. Slonczewski, J. Appl. Phys. **54**, 3370 (1983). See also S. V. Lebedev, C. E. Patton, M. A. Wittenauer, L. V. Saraf, and R. Ramesh, *ibid.* **91**, 4426 (2002).
[46] B. Heinrich, J. F. Cochran, and R. Hasegawa, J. Appl. Phys. **57**, 3690 (1985).
[47] A. Abragam and B. Bleaney, *Electron Paramagnetic Resonance of Transition Ions* (Oxford University Press, Oxford, 1970); J. H. van Vleck and V. F. Weisskopf, Rev. Mod. Phys. **17**, 227 (1945).
[48] S. Tomita, M. Hagiwara, T. Kashiwagi, C. Tsuruta, Y. Matssui, M. Fujii, and S. Hayashi, J. Appl. Phys. **95**, 8194 (2004).
[49] Arguments based on assuming that Eq. (3) is valid can be found in M. Pardavi-Horvath and L. J. Swartzendruber, IEEE Trans. Magn. **35**, 3502 (1999). See also A. F. Kip and R. D. Arnold, Phys. Rev. **75**, 1556 (1949).
[50] D. P. Ray-Chaudhuri, Indian J. Phys. **9**, 383 (1935); L. R. Bickford, Phys. Rev. **78**, 449 (1950); H. Takei and S. Chiba, J. Phys. Soc. Jpn. **21**, 1255 (1966). The gyromagnetic ratio of maghemite γ-Fe_2O_3 was also determined by measurements of the Einstein-de Haas effect in S. J. Barnett and G. S. Kenny, Phys. Rev. **87**, 723 (1952). See also *Ferromagnetic Materials*, edited by E. P. Wohlfarth (North-Holland, Amsterdam, 1980).
[51] M. P. Morales, M. Audres-Verges, S. Veintemillas-Verdaguer, M. I. Montero, and C. J. Serna, J. Magn. Magn. Mater. **203**, 146 (1999).
[52] B. K. Kuanr, R. E. Camley, and Z. Celinski, J. Magn. Magn. Mater. **286**, 276 (2005). See also D. Pain, M. Ledieu, O. Acher, A. L. Adenot, and F. Duverger, J. Appl. Phys. **85**, 5151 (1999); and Y. Liu, L. Chen, C. Y. Tan, H. J. Liu, and C. K. Ong, Rev. Sci. Instrum. **76**, 063911 (2005), i.e., their Eq. (6).
[53] Y. L. Raikher and V. I. Stepanov, Phys. Rev. B **50**, 6250 (1994).
[54] F. Bødker, S. Mørup, and S. Linderoth, Phys. Rev. Lett. **72**, 282 (1994).
[55] G. Herzer, IEEE Trans. Magn. **26**, 1397 (1990). See also G. Herzer, in *Handbook of Magnetic Materials*, edited by K. H. J. Buschow (Amsterdam, The Netherlands, 1997), Vol. 10.
[56] X. Battle and A. Labara, J. Phys. D **35**, R15 (2002).
[57] M. El-Hilo, R. W. Chantrell, and K. O'Grady, J. Appl. Phys. **84**, 5114 (1998).
[58] *Cluster Assembled Materials*, edited by K. Sattler (Trans Tech Publications, Enfield, New Hampshire, 1996).
[59] J. L. Dormann, D. Fiorani, and E. Tronc, Adv. Chem. Phys. **98**, 283 (1997).
[60] J. F. Löffler, H. B. Braun, and W. Wagner, Phys. Rev. Lett. **85**, 1990 (2000).
[61] A. Aharoni, J. Appl. Phys. **69**, 7762 (1991); **81**, 830 (1997). Mention is also made of the more recent study of Arias and coworkers, i.e., R. Arias, P. Chu, and D. L. Mills, Phys. Rev. B **71**, 224410 (2005), concerning the response of a uniformly magnetized ferromagnetic sphere to a spatially inhomogeneous microwave field, under conditions where both dipolar interactions between the spins and exchange couplings enter importantly.
[62] R. Skomski, H. Zeng, and D. J. Sellmyer, IEEE Trans. Magn. **37**, 2549 (2001). See also A. Zangwill, *Physics at Surfaces* (Cambridge University Press, New York, 1988).
[63] R. Ramprasad, P. Zurcher, M. Petras, M. Miller, and P. Renaud, J. Appl. Phys. **96**, 519 (2004). See also C. Brosseau and A. Beroual, Prog. Mater. Sci. **48**, 373 (2003); M. Sahimi, *Heterogeneous Materials I: Linear Transport and Optical Properties* (Springer, New York, 2003); and T. C. Choy, *Effective Medium Theory, Principles and Applications* (Oxford University Press, Oxford, 1999).
[64] J.-C. Bluet, I. Epelboin, and D. Quivy, C. R. Seances Acad. Sci. III **247**, 246 (1958).
[65] S. Redner, *Physics of Finely Divided Matter* (Springer-Verlag, Berlin, 1985).
[66] V. V. Dobrovitski, M. I. Katsnelson, and B. N. Harmon, Phys. Rev. Lett. **90**, 067201 (2003).
[67] See, e.g., *Interfacial Properties on the Submicrometer Scale*, edited by J. Frommer and R. M. Overney (American Chemical Society, Washington, DC, 2000), Vol. 781.
[68] B. Abeles, P. Sheng, M. D. Couts, and Y. Arie, Adv. Phys. **24**, 407 (1975). See also B. Abeles, in *Applied Solid State Science: Advances in Materials and Device Research*, edited by R. Wolfe (Academic, New York, 1976), and references therein.
[69] H. Sher and R. Zallen, J. Chem. Phys. **53**, 3759 (1970). See also M. Sahimi, *Heterogeneous Materials I: Linear Transport and Optical Properties* (Springer-Verlag, New York, 2003).
[70] H. D. Chopra and S. Z. Hua, Phys. Rev. B **66**, 020403(R) (2002).
[71] E. Y. Tsymbal, O. N. Mryasov, and P. R. LeClair, J. Phys.: Condens. Matter **15**, R109 (2003).
[72] *Spin Electronics*, edited by M. Ziese and M. J. Thornton (Springer-Verlag, Berlin, 2001).
[73] A. E. Berkowitz, J. R. Mitchell, M. J. Carey, A. P. Young, S. Zhang, F. E. Spada, F. T. Parker, A. Hütten, and G. Thomas, Phys. Rev. Lett. **68**, 3745 (1992).
[74] M. Viret, D. Vignoles, D. Cole, J. M. D. Coey, W. Allen, D. S. Daniel, and J. F. Gregg, Phys. Rev. B **53**, 8464 (1996).
[75] J. F. Gregg, W. Allen, K. Ounadjela, M. Viret, M. Hehn, S. M. Thompson, and J. M. D. Coey, Phys. Rev. Lett. **77**, 1580 (1996).
[76] Sh.-F. Zhang and P. M. Levy, J. Appl. Phys. **73**, 5315 (1993).
[77] J. Q. Xiao, J. S. Jiang, and C. L. Chien, Phys. Rev. Lett. **68**, 3749 (1992).
[78] J. J. Versluijs, M. A. Bari, and J. M. D. Coey, Phys. Rev. Lett. **87**, 026601 (2001).
[79] K. J. Kirk, J. N. Chapman, S. McVitie, P. R. Atchison, and C. D. W. Wilkinson, J. Appl. Phys. **87**, 5105 (2000).
[80] G. A. Prinz, Science **282**, 1660 (1998). See also G. A. Prinz, J. Magn. Magn. Mater. **200**, 5105 (2000).
[81] S. A Oliver, P. Shi, W. Hu, H. How, S. W. McKnight, N. E. McGruer, P. M. Zavracky, and C. Vittoria, IEEE Trans. Microwave Theory Tech. **49**, 385 (2001).